Mechanisms of Development 155 (2019) 48–59

Contents lists available at ScienceDirect

Mechanisms of Development

journal homepage: www.elsevier.com/locate/mod

Xenopus slc7a5 is essential for notochord function and eye development

Tomohisa Katada, Hiroyuki Sakurai*

Department of Pharmacology and Toxicology, Kyorin University School of Medicine, 6-20-2, Shinkawa, Mitaka, Tokyo 181-8611, Japan

ARTICLE INFO

Keywords:
slc7a5
Amino acid transporter
Neurogenesis
Sonic hedgehog
Xenopus laevis

ABSTRACT

slc7a5 (also known as LAT1), largely accepted as an amino acid transporter, has been shown to play important roles in cancer and developmental processes. Because knockout mice of *Slc7a5* are embryonically lethal due to placental defects, it is difficult to evaluate its role in early development. In this study, expression and function of slc7a5 were evaluated in *Xenopus laevis* embryos that develop without a placenta. Expression of *slc7a5* was detected in the notochord and in the eye and it was not co-localized with *slc3a2*, which helps slc7a5 to localize at the plasma membrane, before the late neurula stage. Loss-of-function experiment with a morpholino antisense oligonucleotide led to defect of neural and non-neural patterning, inhibition of primary neurogenesis, and disruption of eye development. Disruption of neural development and primary neurogenesis was likely due to impaired notochord development as sonic hedgehog (shh) signaling pathway was compromised in slc7a5-inhibited embryos. These results suggest that slc7a5 is required for notochord development and subsequent primary neurogenesis *via* shh/gli signaling and for eye development. These novel developmental roles of slc7a5 appeared to be independent of transport function at least before the late neurula stage.

1. Introduction

SLC7A5 (solute carrier family 7 member 5, widely accepted as LAT1) is an amino acid transporter initially identified by two groups, Kanai et al. (in rat C6 glioma cells) and Mastroberardino et al. (in human) in 1998 (Kanai et al., 1998; Mastroberardino et al., 1998). It localizes to the plasma membrane accompanied by a type II membrane protein, SLC3A2 (also called 4F2hc or CD98) (Mastroberardino et al., 1998; Nakamura et al., 1999) and contributes to uptake of large neutral amino acids (*e.g.* leucine or phenylalanine) into cells in a sodium ion-independent manner (Kanai et al., 1998; Mastroberardino et al., 1998; Prasad et al., 1999).

Although *SLC7A5* is expressed in various normal tissues, such as the brain and placenta in humans and rodents (Chrostowski et al., 2009; Kanai et al., 1998; Prasad et al., 1999), it has been shown to be expressed in tumor cells and its degree of expression is more prominent as the tumor evolves to a more malignant phenotype (Sakata et al., 2009; Yanagisawa et al., 2012). As its substrates, especially leucine, are shown to stimulate mTOR (mammalian target of rapamycin) pathway and lead to tumor cell proliferation (Kimball and Jefferson, 2004), SLC7A5 can be a novel target for cancer therapy. In fact, several reports including ours have been published showing that inhibition of this transporter by BCH (2-aminobicyclo-(2,2,1)-heptane-2-carboxylic acid) or JPH203 ((*S*)-2-amino-3-(4-((5-amino-2-phenylbenzo[*d*]oxazol-7-yl) methoxy)-3,5-dichlorophenyl)-propanoic acid) represses the proliferation of tumor cells *in vitro* or *in vivo* (Cormerais et al., 2016; Kim et al., 2008; Oda et al., 2010; Rosilio et al., 2015; Ueno et al., 2016; Yun et al., 2014). In addition to tumor cells, it has been shown that SLC7A5 is highly expressed in fetal tissues. For example, Nakada et al. have shown that SLC7A5 is detected in the cardiac muscle, hepatocyte and thymic epithelial cells in human fetuses but not in the respective adult tissues (Nakada et al., 2014). Taken together, it seems that amino acid uptake by SLC7A5 is important for cell proliferation both in malignant tumors and normal development.

We were interested in elucidating a role for SLC7A5 in normal developmental processes. Specifically, we would like to know whether perturbation of SLC7A5 only leads to slower growth or more profound effects during organogenesis. Recently, 3 groups have reported that complete loss of Slc7a5 function leads to embryonic lethality in mice (Ohgaki et al., 2017; Poncet et al., 2014; Sinclair et al., 2013), suggesting that Slc7a5 is essential for early developmental processes. Ohgaki et al. have shown that labyrinth development is disrupted in the $Slc7a5^{-/-}$ placenta and that the $Slc7a5^{-/-}$ embryos were smaller in size than $Slc7a5^{+/-}$ siblings (Ohgaki et al., 2017). Because *Slc7a5* affects placental function, it is impossible to evaluate organogenesis in mouse embryos unless *Slc7a5* knockout with placenta-specific rescue is performed.

Instead of making such mice, we chose to evaluate its function in

* Corresponding author.
E-mail address: hsakurai@ks.kyorin-u.ac.jp (H. Sakurai).

https://doi.org/10.1016/j.mod.2019.01.001
Received 10 September 2018; Received in revised form 26 December 2018; Accepted 3 January 2019
Available online 06 January 2019
0925-4773/

```
slc7a5.S(LAT1a) MAAGSVKRRQSGASKMEEEDRQAAEKMLHQNGSAEPTGSNGGTVELQRTITLVNGVAIIV 60
slc7a5.L(LAT1b) MAADSVKRRQSGASKTEEEDRQAAEKMLHQNGNAEPKSGDGAAVELQRTITLVNGVAIIV 60
                ***.*********** ***************.***....*..***************

slc7a5.S(LAT1a) GTIIGSGIFVTPTGVLREAGSPGLSLLIWAVCGLFSIVGALCYAELGTTISKSGGDYAYV 120
slc7a5.L(LAT1b) GTIIGSGIFVTPTGVLREAGSPGLSLLVWAVCGLFSIVGALCYAELGTTISKSGGDYAYV 120
                *************************.******************************

slc7a5.S(LAT1a) LEVYGALPAFLKLWVELLIIRPSSQYIVALVFATYLLKPVFPTCPVPDDAAKLVACLCIL 180
slc7a5.L(LAT1b) LEVYGALPAFLKLWVELLIIRPSSQYIVALVFATYLLKPVFPTCPVPDDAAKIVACLCIL 180
                *************************************************.*******

slc7a5.S(LAT1a) LLTAINCYSVKAATRVQDAFAAAKLLALCLIIILGFVQLGKGDVENLKPENAFKGTSTNV 240
slc7a5.L(LAT1b) LLTAINCYSVKAATRVQDAFAAAKLLALLLIIILGFVQLGKGGVEDLKPERSFEGTSTNV 240
                *************************** ************.**.****..*.******

slc7a5.S(LAT1a) GQWVLALYSGLFAYGGWNYLNFVVEEMIEPFKNLPRAIIISMPIVTLVYVLTNLAYFTTL 300
slc7a5.L(LAT1b) GQWVLALYSGLFAYGGWNYLNFVVEEMIEPYKNLPRAIIISMPIVTLVYVLTNLAYFTTL 300
                ****************************.****************************

slc7a5.S(LAT1a) SPEQMLNSEAVAVDFGNYHLGVMAWIIPVFVGLSCFGSVNGSLFTSSRLFFVGAREGHLP 360
slc7a5.L(LAT1b) TPEQMLNSEAVAVDFGNYHLGVMAWIIPVFVGLSCFGSVNGSLFTSSRLFFVGAREGHLP 360
                .************************************************************

slc7a5.S(LAT1a) SLLAMIHPRLLTPMPSLIFTCAMTLLYAFSDDIFSVINFFSFFNWLCVALAIIGMMWLRY 420
slc7a5.L(LAT1b) SLLAMIHPRLLTPMPSLIFTCAMTLLYAFSDDIFSVINFFSFFNWLCVALAIIGMMWLRY 420
                ************************************************************

slc7a5.S(LAT1a) KKPELERPIKVNILLPIFFILACIFLIVVSFYMTPVECGIGFIIVLSGVPVYFFGVWWQK 480
slc7a5.L(LAT1b) KKPELERPIKVNILLPIFFILACIFLIVVSFYMTPVECGIGFIIILTGVPVYFFGVWWQN 480
                *******************************************.*.************.

slc7a5.S(LAT1a) KPDWLLHGIHSSTALLQKVMEAVPQES 507
slc7a5.L(LAT1b) KPDWILHGIHSSTALLQKVMEAVPQES 507
                ****.**********************
```

Fig. 1. Comparison of amino acid sequences between slc7a5.S and slc7a5.L in *Xenopus laevis*.
Two amino acid sequences, slc7a5.S (NM_001096373) and slc7a5.L (NM_001090065), were aligned by clustalW. Asterisks represent identical amino acid residues. Dots show similar residues. Shaded cysteine is predicted to be participated in a disulfide bond with slc3a2 (4F2hc or CD98) protein.

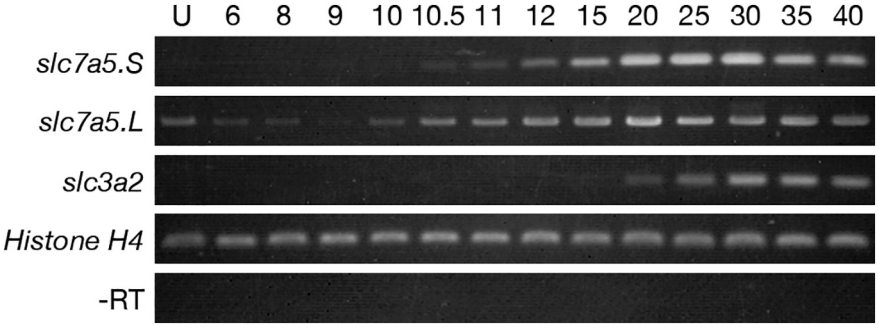

Fig. 2. Temporal expression of *slc7a5.S* and *slc7a5.L* in the developmental stages.
Semi-quantitative RT-PCR was performed to examine the expression of *slc7a5* mRNA in the developmental stages. *slc7a5.S* started to express from the gastrula stage (st.10.5) and increased thereafter. *slc7a5.L* expression was found maternally and also detected in the zygotic stage. *slc3a2* (*4F2hc* or *CD98*) expression was detected from st.20. *Histone H4* was used as a loading control. −RT represents a negative control without reverse transcriptase. Numbers show developmental stages defined by Nieuwkoop and Faber (1994). U: unfertilized egg.

embryos of *Xenopus laevis* that develops without a placenta. *Xenopus* orthologs of *SLC7A5* were detected in the eye and notochord starting at the neurula stage. Its functional disruption by a morpholino antisense oligonucleotide (MO) affected early neural and non-neural patterning, primary neurogenesis and eye development. These phenotypes can be caused, at least partially, by notochord malfunction that led to decreased shh/gli signaling.

2. Material and methods

2.1. Embryos

Xenopus laevis eggs were obtained by injecting 300–500 unit of human chorionic gonadotropin, Gonatropin (Aska Pharmaceutical, Tokyo, Japan) to adult female and were fertilized artificially with sperm from adult male. Embryos were dejellied with 1% sodium mercaptoacetate (pH 10) and cultured in 0.1xMMR (Marc's Modified Ringers; 10 mM NaCl, 0.2 mM KCl, 0.1 mM $MgCl_2$, 0.2 mM $CaCl_2$, 0.5 mM HEPES, pH 7.5). Stages were determined according to normal table of *Xenopus laevis* (Nieuwkoop and Faber, 1994).

2.2. RT-PCR

Total RNA extraction was performed with ISOGEN (NIPPON GENE, Tokyo, Japan) and reverse transcription was carried out with SuperScript III (Thermo Fisher Scientific, Yokohama, Japan) using

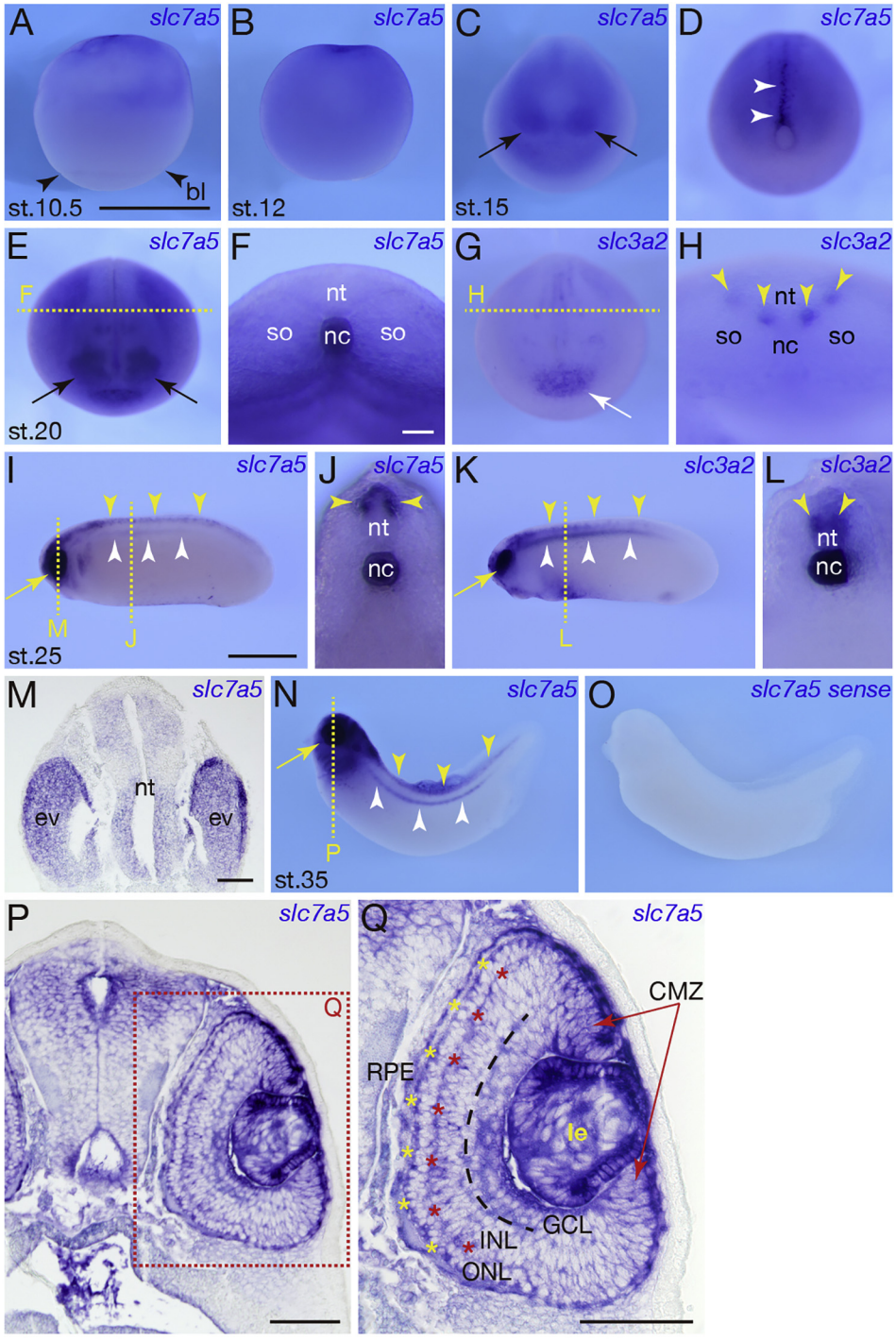

Fig. 3. Spatial expression of *slc7a5.S* and *slc3a2* in the developmental stages.
Whole-mount *in situ* hybridization was performed to analyze spatial expression of *slc7a5.S* (shown in A–F, I, J, M–Q) and *slc3a2* (shown in G, H, K and L) in the developmental stages. (A) st.10.5. Lateral view. *slc7a5.S* expressed in the animal hemisphere. Black arrowheads indicate the blastopore lip (bl). (B) st.12. Lateral view. *slc7a5.S* expression was observed throughout the animal hemisphere at st.10.5. (C, D) st.15. (C) Anterior view. *slc7a5.S* localized at the eye anlagen (black arrows). (D) Posterior view. *slc7a5.S* was detected in the notochord from the blastopore to anterior along midline as indicated by white arrowheads. (E–H) st.20. (E) Anterior view. More definite expression of *slc7a5.S* was detected at the eye field in comparison to st.15 embryo in (C) (black arrows). A yellow broken line indicates the plane of section in panel (F). (F) Transverse section of st.20 embryo shown in panel (E). Strong expression of *slc7a5.S* was observed in the notochord (nc). (G) Anterior view. Weak expression of *slc3a2* was detected in the cement grand (white arrow). A yellow broken line indicates the plane of section in panel (H). (H) Transverse section of st.20 embryo shown in panel (G). Spotted expression of *slc3a2* was observed in the neural tube (yellow arrowheads), but no expression was detected in the notochord unlike *slc7a5.S* expression in st.20 embryo. (I–L) st.25. (I) Lateral view. *slc7a5.S* expression was intensely detected in the eye (yellow arrow) and also observed in the neural tube (yellow arrowheads) and the notochord (white arrowheads). Two yellow broken lines represent the plane of section in panel (J) and (M). (J) Transverse section of st.25 embryo at trunk region shown in panel (I). *slc7a5.S* was observed in the dorsal part of the neural tube (nt, yellow arrowheads) and the notochord (nc). (K) Lateral view. *slc3a2* expression was intensely detected in the eye (yellow arrow) and also observed in the neural tube (yellow arrowheads) and the notochord (white arrowheads) as *slc7a5.S* expression shown in panel (I). (L) Transverse section of st.25 embryo shown in panel (K). *slc3a2* was observed in the ventral part of the neural tube (nt, yellow arrowheads) and the notochord (nc). (M) Transverse section of st.25 embryo at trunk region shown in panel (I). *slc7a5.S* expressed in the eye vesicle (ev) and the neural tube (nt). (N–Q) st.35. (N) Lateral view. *slc7a5.S* expression was maintained in the eye (yellow arrow), the neural tube (yellow arrowhead) and the notochord (white arrowhead). A yellow broken line indicates the plane of section in panel (P). (O) Negative control with a sense probe of *slc7a5.S*. (P) Transverse section of st.35 embryo. A rectangle with red broken line represents a region magnified in panel (Q). (Q) Higher magnification of photomicrograph of rectangle (Q) in panel (P). *slc7a5.S* expressed in the lens (le), CMZ of the neural retina (red arrow), the border of INL and ONL (red asterisks) and RPE (yellow asterisks). Scale bars: 1 mm in A–E and G; 0.1 mm in F, H, J and L; 1 mm in I, K, N and O; 0.1 mm in M; 0.1 mm in P; 0.1 mm in Q. bl: blastopore lip, CMZ: ciliary marginal zone of the neural retina, ev: eye vesicle, nc: notochord, nt: neural tube, so: somite, GCL: ganglion cell layer, INL: inner nuclear layer, le: lens, ONL: outer nuclear layer, RPE: retinal pigment epithelium. (For interpretation of the references to color in this figure legend, the reader is referred to the web version of this article.)

0.1 μg of total RNA and oligo dT primer. Sequences of primer sets and cycle numbers were as follows: *slc7a5.S* forward, 5′-CAA CAA CCA CAA ACT ATT GC-3′; *slc7a5.S* reverse, 5′-CAA GTT AAG GCA ACA TGT AG-3′ (27 cycles); *slc7a5.L* forward, 5′-CAC AAA GTT CAT CTC TGT T-3′; *slc7a5.L* reverse, 5′-CAA ACA GAA AGG TAT AAG AG-3′ (29 cycles); *slc3a2* forward, 5′-CCT GCT CAG TCC TCA AGA CC-3′; *slc3a2* reverse, 5′-TCA TTC TGG TCC CAG CTT CT-3′ (26 cycles); *Histone H4* forward, 5′-CGG GAT AAC ATT CAG GGT ATC ACT-3′; *Histone H4* reverse, 5′-ATC CAT GGC GGT AAC TGT CTT CCT-3′ (27 cycles). Negative control (−RT) was performed without reverse transcriptase. All cycle numbers are within the linear range of amplification.

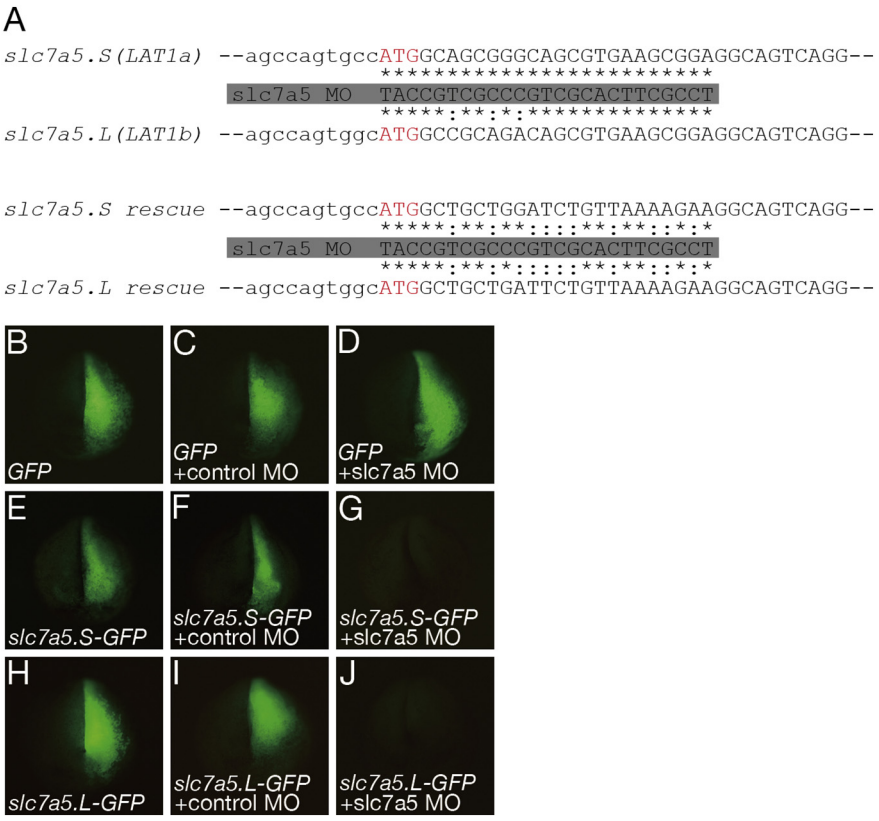

Fig. 4. slc7a5 MO specifically inhibits translation of *slc7a5.S* and *slc7a5.L* mRNA.
(A) The sequence of slc7a5 MO used in this study. slc7a5 MO completely matches to *slc7a5.S*, but has three mismatches to *slc7a5.L*. Two rescue forms, *slc7a5.S rescue* and *slc7a5.L rescue*, have 10 or 11 mismatches to slc7a5 MO with silent mutations. ATG in red represents a start codon and double dots represent the mismatch of the base. (B–J) Validation assay of slc7a5 MO with GFP fusion constructs, *slc7a5.S-GFP* and *slc7a5.L-GFP*. *GFP* construct (0.5 ng) with or without MO (20 ng) was injected into dorsoanimal region of 4-cell stage embryos. GFP fluorescence was observed in the embryos injected with *GFP* only or *GFP* and control MO, but slc7a5 MO abolished the fluorescence in both *slc7a5.S-GFP* and *slc7a5.L-GFP* co-injection. (For interpretation of the references to color in this figure legend, the reader is referred to the web version of this article.)

2.3. RT-qPCR

Total RNA extraction from slc7a5 MO- or control MO-injected embryos (both sides) at st.15 was performed with ISOGEN (NIPPON GENE, Tokyo, Japan) and reverse transcription was carried out with SuperScript III (Thermo Fisher Scientific, Yokohama, Japan) using 0.1 μg of total RNA and oligo dT primer. Sequences of primer sets were as follows: *chrd.1* forward, 5′-TGG ATG GTC TGC ACA ATG TT-3′; *chrd.1* reverse, 5′-GAA TCC AAG GTG GCA AGG TA-3′; *shh* forward, 5′-GCA CCA GGT CGT TCA AGT CT-3′; *shh* reverse, 5′-GGC AGT TAG AGG CGC ATA AG-3′; *ptch2* forward, 5′-GCC AGC AAG GAT CCA AAT TA-3′; *ptch2* reverse, 5′-CTT CTG CTC TTG GCA GGT TC-3′; *foxa2* forward, 5′-TCA TGG ACC TGT TCC CTT TC-3′; *foxa2* reverse, 5′-GAA TCA GGG TGT AGG GTC CA-3′; *gli1* forward, 5′-ACC AAC AGT GGG GAT GAT GT-3′; *gli1* reverse, 5′-TCT TGA GAG CTT GGG CTC AT-3′; *gli2* forward, 5′-CTC CAT GCT CAC AAC ATT GG-3′; *gli2* reverse, 5′-CCC AGG ACC CTA ACG TCT TT-3′; *Histone H4* forward, 5′-TAT CAC TAA ACC CGC CAT CC-3′; *Histone H4* reverse, 5′-TCT TCC TCT TGG CGT GTT CT-3′. Reaction was performed with SYBR Select Master Mix and 7300 Real Time PCR System (Applied Biosystems) according to the manufacturer's instruction. The data was analyzed using 7300 System Sequence Detection Software Version 1.4.

2.4. Whole-mount in situ hybridization

Whole-mount *in situ* hybridization was performed as described previously (Katada and Sakurai, 2016). Briefly, the method of Shain and Zuber was employed (Shain and Zuber, 1996) and embryos after signal detection were bleached with a solution containing hydrogen peroxide (Koga et al., 2007; Mayor et al., 1995). *slc7a5.S*, *slc3a2.L*, *shh*, *ptch2*, *foxa2* (also known as *HNF-3β*), *gli1* and *gli2* were obtained by PCR cloning using following primer sets after reverse transcription of total RNAs from *Xenopus* embryos and these amplified PCR fragments were subcloned into *pBIISK+* vector.

slc7a5.S forward, 5′-GGG GGA TCC ATG GCA GCG GGC AGC GTG AA-3′; *slc7a5.S* reverse, 5′-GGG CTC GAG TTA AGA CTC CTG AGG GAC AG-3′; *slc3a2.L* forward, 5′-GGG GAA TTC CAA GAC ACC AGG ACT CCG AC-3′; *slc3a2.L* reverse, 5′-GGG CTC GAG TTA TCC ACT ATA AGG GTA TT-3′; *shh* forward, 5′-GGG GGA TCC ATG CTG GTT GCG AAC TCG AA-3′; *shh* reverse, 5′-GGG GAA TTC TCA ACT GGA TTT CGT TGC CA-3′; *ptch2* forward, 5′-GGG CTC GAG CCG AAA CCA ACG TTC AGT AC-3′; *ptch2* reverse 5′-GGG TCT AGA CTA GTG TTG AAC AGA CAA GT-3′; *foxa2* forward, 5′-GGG GAA TTC ATG CTT GGG GCT GTG AAA AT-3′; *foxa2* reverse, 5′-GGG CTC GAG CAT GGG ACA GGA CAG AAT GG-3′; *gli1* forward, 5′-GGG GAA TTC TGT GAT TAC CAA GGG CAA CA-3′; *gli1* reverse, 5′-GGG CTC GAG ACA TTG TGT TTA GGT ACT TA-3′; *gli2* forward, 5′-GGG GGA TCC GTC TGT ACA GAG GAA TAT CA-3′; *gli2* reverse, 5′-GGG GAA TTC TTA GGA CAT CAG ATT GAG AA-3′. *sox2*, *xk81a1*, *tubb2b*, *chrd.1* and *pax6* are kind gifts from Dr. Tsutomu Kinoshita (Rikkyo University, Tokyo). The antisense probes for *slc7a5.S* (*Bam*HI/T7), *slc3a2.L* (*Eco*RI/T7) *sox2* (*Eco*RI/T7), *xk81a1* (*Eco*RI/SP6), *tubb2b* (*Bam*HI/T3), *chrd.1* (*Eco*RI/T7), *shh* (*Bam*HI/T7), *ptch2* (*Xho*I/T3), *foxa2* (*Eco*RI/T7), *gli1* (*Eco*RI/T7), *gli2* (*Bam*HI/T7) and *pax6* (*Eco*RI/T7) were prepared with restriction enzyme and RNA polymerase shown in the parenthesis in presence of digoxygenin-UTP (Röche Diagnostics).

2.5. Histology

Embryos after whole-mount *in situ* hybridization were dehydrated and embedded in paraffin, Parabett (Muto Pure Chemicals, Tokyo, Japan). Sections were cut at 10 μm. Slides were deparaffinized and mounted with 50% glycerol in PBS. For hematoxylin and eosin staining, sections were cut at 10 μm and slides were processed according to the manufacturer's instruction (Wako Pure Chemical Industries, Osaka, Japan).

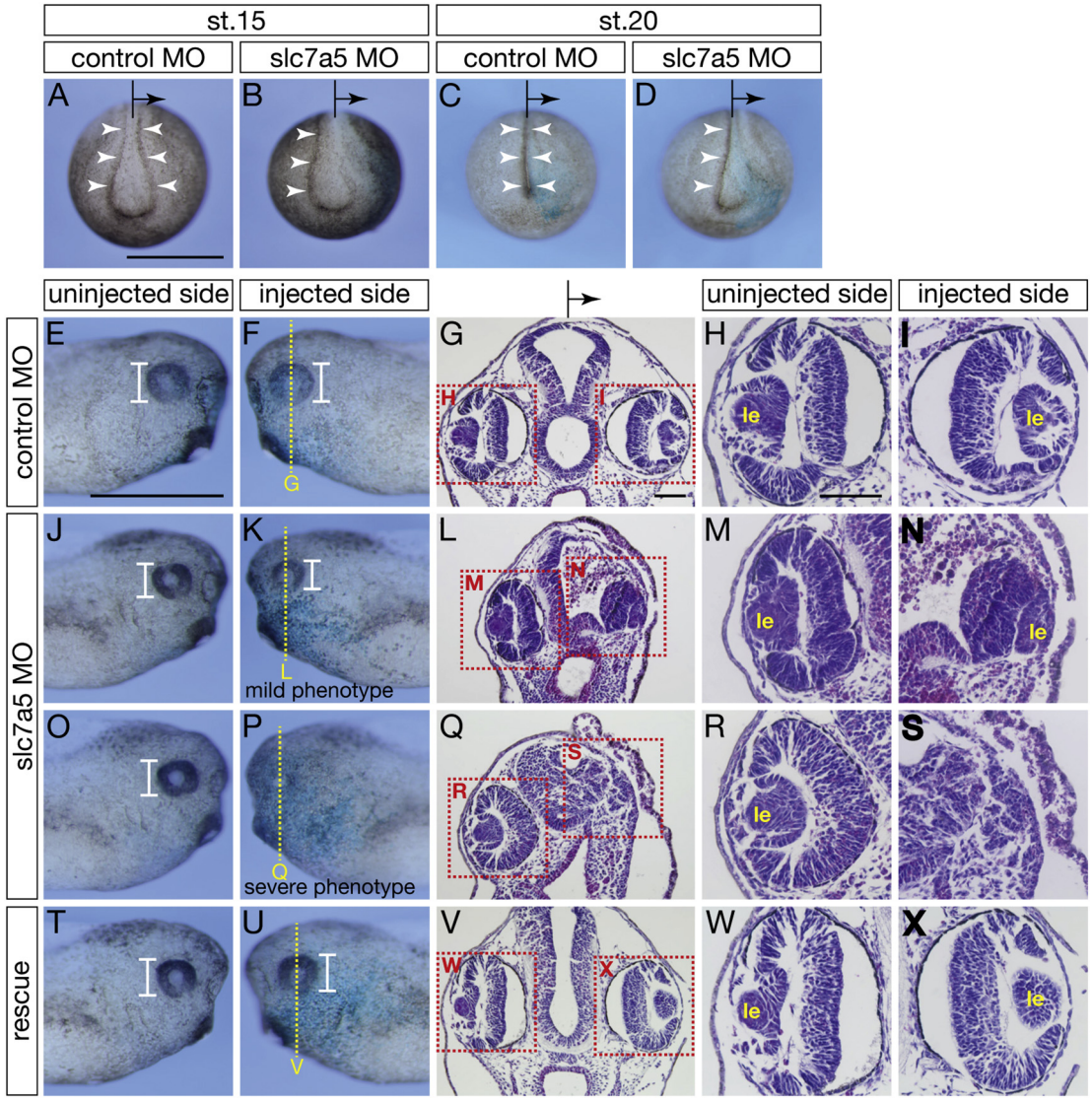

Fig. 5. slc7a5 depletion impaired neural tube closure and eye development.
Loss-of-function experiment was performed with slc7a5 MO. (A, B) st.15 embryo. Anterior view. White arrowheads represent the neural fold. (A) Control MO-injected embryo. (B) slc7a5 MO-injected embryo. The neural fold in the injected side was not distinct compared with that in the uninjected side. (C, D) st.20 embryo. Anterior view. White arrowheads show the neural fold. (C) Control MO-injected embryo. (D) slc7a5 MO-injected embryo. The neural fold in the injected side did not fuse at the midline and neural tube closure was not seen in the injected side. (E–X) st.35 embryo. (E–I) Control MO-injected embryo. (E) Uninjected side of control MO. (F) Injected side of control MO. Yellow broken line shows the plane of section in panel (G). (G) Transverse section of control MO-injected embryo. Two rectangles with red broken line represent regions magnified in panel (H) and (I). (H, I) Higher magnification of photomicrograph of rectangle (H) and (I) in panel (G). (J–S) Embryos injected with slc7a5 MO. (J–N) Mild phenotype. (J) Uninjected side of slc7a5 MO-injected embryo. (K) Injected side of slc7a5 MO-injected embryo. Yellow broken line shows the plane of section in panel (L). (L) Transverse section of slc7a5 MO-injected embryo with small eye. Two rectangles with red broken line represent regions magnified in panel (M) and (N). (M, N) Higher magnification of photomicrograph of rectangle (M) and (N) in panel (L). (O–S) Severe phenotype. (O) Uninjected side of slc7a5 MO-injected embryo. (P) Injected side of slc7a5 MO-injected embryo. Yellow broken line shows the plane of section in panel (Q). (Q) Transverse section of slc7a5 MO-injected embryo with no apparent eye. Two rectangles with red broken line represent regions magnified in panel (R) and (S). (R, S) Higher magnification of photomicrograph of rectangle (R) and (S) in panel (Q). (T–X) Rescue by coinjection of *slc7a5.S* mRNA and *slc7a5.L* mRNA with slc7a5 MO. (T) Uninjected side (*i.e.* no rescue). (U) Injected side of rescue constructs. Eye structure was rescued. Yellow broken line shows the plane of section in panel (V). (V) Transverse section of rescue constructs-injected embryo. Two rectangles with broken line represent regions magnified in panel (W) and (X). (W, X) Higher magnification of photomicrograph of rectangle (W) and (X) in panel (V). Arrow indicates the injected side. White brackets indicate the size of the eye. *β-Galactosidase* mRNA (1 ng) was used as a tracer (blue). Scale bars: 1 mm in A–D; 1 mm in E, F, J, K, O, P, T, U; 0.1 mm in G, L, Q, V; 0.1 mm in H, I, M, N, R, S, W, X. le: lens. (For interpretation of the references to color in this figure legend, the reader is referred to the web version of this article.)

2.6. Morpholino antisense oligonucleotide (MO) or overexpression of slc7a5 in Xenopus embryos

Morpholino antisense oligonucleotides (MO) were purchased from Gene Tools (OR, USA). Sequences of slc7a5 MO and control MO were as follows; slc7a5 MO, 5′-TCC GCT TCA CGC TGC CCG CTG CCA T-3′; control MO, 5′-CCT CTT ACC TCA GTT ACA ATT TAT A-3′. Total injected amount of MO was 20 ng in all experiments. To verify the inhibitory effect of slc7a5 MO, GFP fusion constructs, *slc7a5.S-GFP* and *slc7a5.L-GFP*, were prepared by inserting *slc7a5.S* and *slc7a5.L* in frame into *pCS2mt-UGP* vector, respectively. Sequences of primers for GFP fusion constructs were as follows; *slc7a5.S-GFP* forward, 5′-GGG GGA TCC AGG CGA AGC CAG TGC CAT GGC AGC GGG CAG CGT G-3′; *slc7a5.S-GFP* reverse, 5′-GGG TCT AGA AGA CTC CTG AGG GAC AGC

Table 1
Effect of slc7a5 depletion on *Xenopus* development. Chi-square test was performed between two kinds of injected samples, control MO (20 ng) and slc7a5 MO (20 ng) or slc7a5 MO (20 ng) and slc7a5 MO (20 ng) + *slc7a5.S* (2 ng) + *slc7a5.L* (2 ng) and found to be significant, $p < 0.01$.

st.20

Injected sample	Normal	Left-right asymmetry	Total embryos
Control MO 20 ng	117 (100%)	0 (0%)	117
slc7a5 MO 20 ng	12 (12%)	92 (88%)	104

st.35

Injected sample	Normal	Mild phenotype	Severe phenotype	Total embryos
Control MO 20 ng	103 (98%)	2 (2%)	0 (0%)	105
slc7a5 MO 20 ng	18 (15%)	87 (72%)	16 (13%)	121
slc7a5 MO 20 ng + *slc7a5.S* 2 ng + *slc7a5.L* 2 ng	57 (48%)	57 (48%)	4 (3%)	118

Table 2
Effect of slc7a5 depletion on *pax6* and *nrl* expression at st.35. Chi-square test was performed between two kinds of injected samples, control MO (20 ng) and slc7a5 MO (20 ng) or slc7a5 MO (20 ng) and slc7a5 MO (20 ng) + *slc7a5.S* (2 ng) + *slc7a5.L* (2 ng), and found to be significant, $p < 0.01$.

pax6

Injected sample	Normal	Reduced	Total embryos
Control MO 20 ng	64 (100%)	0 (0%)	64
slc7a5 MO 20 ng	9 (10%)	84 (90%)	93
slc7a5 MO 20 ng + *slc7a5.S* 2 ng + *slc7a5.L* 2 ng	38 (50%)	38 (50%)	76

nrl

Injected sample	Normal	Reduced	Total embryos
Control MO 20 ng	63 (100%)	0 (0%)	63
slc7a5 MO 20 ng	12 (14%)	76 (86%)	88
slc7a5 MO 20 ng + *slc7a5.S* 2 ng + *slc7a5.L* 2 ng	32 (46%)	38 (54%)	70

CT-3′; *slc7a5.L-GFP* forward, 5′-GGG ATC GAT CCA TCC AAA GCC AGT GGC ATG GCC GCA GAC AGC GTG-3′; *slc7a5.L-GFP* reverse, 5′-GGG TCT AGA GGA CTC CTG GGG GAC AGC CT-3′. For rescue experiments, rescue plasmids were constructed by inserting *slc7a5.S* and *slc7a5.L* with silent mutations in MO-binding domain into *pCS2+* vector, respectively. Sequences of primers for rescue constructs were as follows; *slc7a5.S-rescue* forward, 5′-GGG GGA TCC ATG GCT GCT GGA TCT GTT AAA AGA AGG CAG TCA GGA-3′; *slc7a5.S-rescue* reverse, 5′-GGG CTC GAG TTA AGA CTC CTG AGG GAC AG-3′; *slc7a5.L-rescue* forward, 5′-GGG ATC GAT ATG GCT GCT GAT TCT GTT AAA AGA AGG CAG TCA GGA-3′; *slc7a5.L-rescue* reverse, 5′-GGG TCT AGA TTA GGA CTC CTG GGG GAC AG-3′. For overexpression experiments, plasmids were constructed by inserting wild-type of *slc7a5.S* and *slc7a5.L* into pCS2+ vector, respectively. Sequences of primers for overexpression constructs were as follows; *slc7a5.S-oe* forward, 5′-GGG GGA TCC ATG GCA GCG GGC AGC GTG AA-3′; *slc7a5.S-oe* reverse, 5′-GGG CTC GAG TTA AGA CTC CTG AGG GAC AG-3′; *slc7a5.L-oe* forward, 5′-GGG ATC GAT ATG GCC GCA GAC AGC GTG AA-3′; *slc7a5.L-oe* reverse, 5′-GGG TCT AGA TTA GGA CTC CTG GGG GAC AG-3′.

All capped RNAs were synthesized with SP6 RNA polymerase. *β-Galactosidase* RNA was produced from *pCMV-SPORT β-gal* (Thermo Fisher Scientific, Yokohama, Japan). Microinjection was performed using NANOJECT II Kit (Drummond Scientific Company) and RNAs and/or MOs were unilaterally injected to dorsoanimal region of 4-cell stage embryos and uninjected side was defined as a control side.

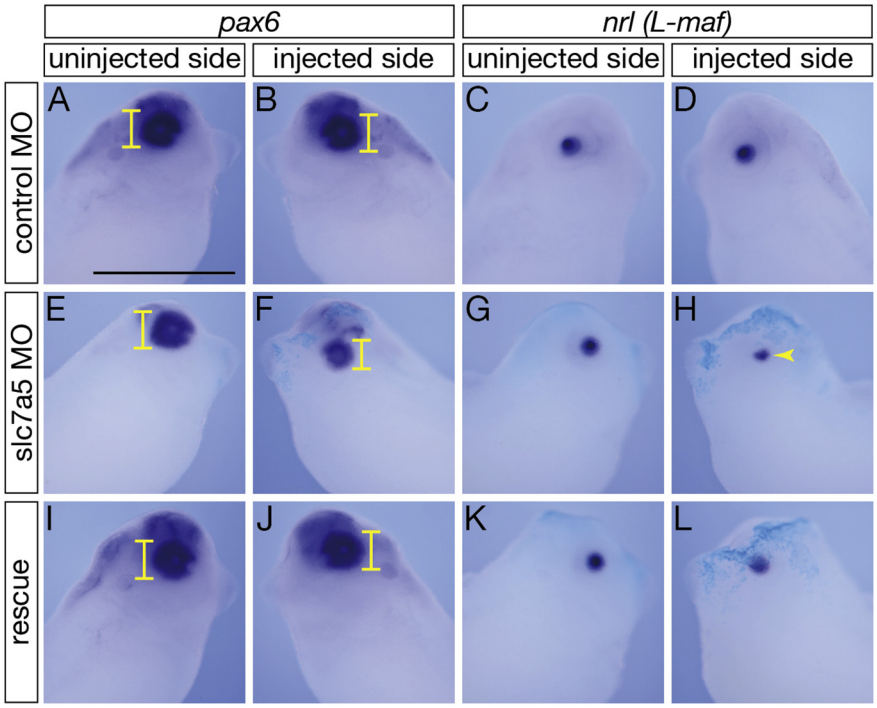

Fig. 6. Depletion of slc7a5 showed decrease of *pax6* and *nrl* (*L-maf*) in eye development.
Eye structure was investigated in slc7a5-depleted embryo by whole-mount *in situ* hybridization with *pax6* and *nrl* (*L-maf*) probes. (A–D) Control MO-injected embryo. (A, B) *pax6* expression in control MO-injected embryo. (A) Uninjected side of control MO-injected embryo. (B) Injected side of control MO-injected embryo. (C, D) *nrl* (*L-maf*) expression in control MO-injected embryo. (C) Uninjected side of control MO-injected embryo. (D) Injected side of control MO-injected embryo. (E–H) slc7a5 MO-injected embryo. (E, F) *pax6* expression in slc7a5 MO-injected embryo. (E) Uninjected side of slc7a5 MO-injected embryo. (F) Injected side of slc7a5 MO-injected embryo. *pax6* expression was repressed. (G, H) *nrl* (*L-maf*) expression in slc7a5 MO-injected embryo. (G) Uninjected side of slc7a5 MO-injected embryo. (H) Injected side of slc7a5 MO-injected embryo. *nrl* (*L-maf*) expression was decreased. (I–L) Rescue effect in coinjection of *slc7a5.S* mRNA and *slc7a5.L* mRNA with slc7a5 MO. (I, J) *pax6* expression in rescue constructs-injected embryo. (I) Uninjected side of rescue constructs-injected embryo. (J) Injected side of rescue constructs-injected embryo. *pax6* expression was rescued. (K, L) *nrl* (*L-maf*) expression in rescue contents-injected embryo. (K) Uninjected side of rescue constructs-injected embryo. (L) Injected side of rescue constructs-injected embryo. *nrl* (*L-maf*) expression was rescued. Yellow brackets indicate the size of the eye. *β-Galactosidase* mRNA (1 ng) was used as a tracer (blue). Scale bars: 1 mm. (For interpretation of the references to color in this figure legend, the reader is referred to the web version of this article.)

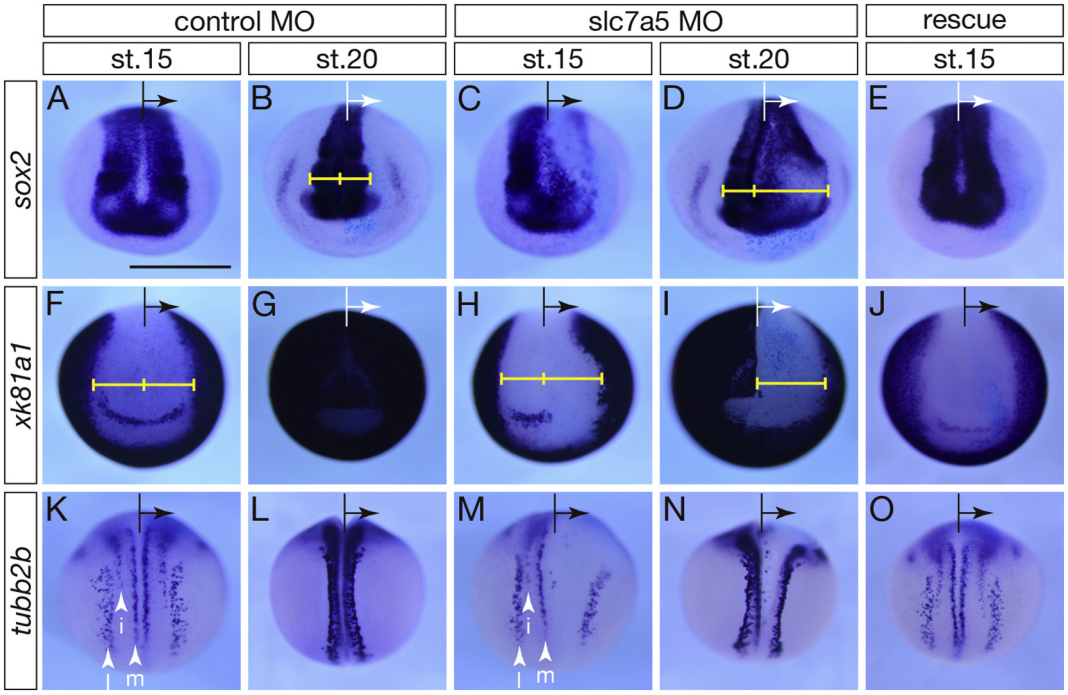

Fig. 7. Inhibition of slc7a5 led to the disorganization of neural- and non-neural patterning and primary neurogenesis.
Neurula stage embryos (st.15 and st.20) were surveyed to analyze neural- and non-neural patterning in slc7a5-depleted embryos. Whole-mount *in situ* hybridization was performed with *sox2*, *xk81a1*, *tubb2b* (*N-tubulin*) probes in embryos injected with control MO or slc7a5 MO. Black and white arrow represents the injected side. Yellow brackets indicate the width of the neural region in the embryo. (A–E) *sox2* expression. Anterior view. Broader expression domain was observed in slc7a5 MO-injected side. (F–J) *xk81a1* expression. Anterior view. *xk81a1*-negative domain was observed in the anterior part of slc7a5 MO-injected side even after st.20. (K–O) *tubb2b* expression. Dorsal view. Motoneuron in medial region and interneuron in more lateral region were eliminated in slc7a5 MO-injected embryo. (E, J, O) Coinjection of *slc7a5.S* and *slc7a5.L* mRNA with slc7a5 MO rescued these phenotypes. *β-Galactosidase* RNA (1 ng) was used as a tracer. Scale bars: 1 mm. l: lateral neurons (sensory neurons or Rohon-Beard neurons), i: intermediate neurons (interneurons), m: medial neurons (motoneurons). (For interpretation of the references to color in this figure legend, the reader is referred to the web version of this article.)

2.7. Statistical analysis

All results shown in four tables were analyzed by Chi-square test and $p < 0.01$ was considered statistically significant.

3. Results

3.1. Spatiotemporal expression of slc7a5 in Xenopus laevis embryos

Two *Xenopus* orthologs of *SLC7A5* gene were found in Xenbase: *slc7a5.S* (NM_001096373) and *slc7a5.L* (NM_001090065). We successfully isolated both mRNAs from total RNAs of st.35 embryos. The cysteine residue responsible for the disulfide bridge with slc3a2 was predicted by comparison of slc7a5.S and slc7a5.L with human SLC7A5 (Wagner et al., 2001) (Fig. 1). By RT-PCR, *slc7a5.S* started to express at the gastrula stage (st.10.5) while *slc7a5.L* was already present in the unfertilized egg. Expression levels of these genes gradually increased through neurula stages. To our surprise, expression of *slc3a2* mRNA was only observed from st.20 (late neurula) on (Fig. 2). By whole-mount *in situ* hybridization, *slc7a5.S* was expressed throughout animal side of embryos during gastrula stages (Fig. 3A, B). During neurula stages, *slc7a5.S* expression was detected in the eye field (Fig. 3C) and the notochord extending from the blastopore to the anterior side (Fig. 3D). Compared with st.15 embryos, more distinct and stronger expression of the gene was noted in the eye field at st.20 (Fig. 3E). Expression of *slc7a5.S* in the notochord at st.20 was confirmed in the transverse section (Fig. 3F). Interestingly, *slc3a2* was detected in the cement grand (Fig. 3G) and the neural tube (Fig. 3H), but not in the eye field or notochord at this stage. Coexpression of *slc7a5.S* and *slc3a2* was observed in the eye at st.25 (Fig. 3I, K, M). Transverse sections showed both genes were detected in the notochord, however, *slc7a5.S* was found in the dorsal part of the neural tube while *slc3a2* was detected in the ventral part of it (Fig. 3J, L). Expression of *slc7a5.S* in the eye, notochord and neural tube was maintained at st.35 (Fig. 3N). Expression of *slc7a5.S* was detected in the lens, the cilliary marginal zone (CMZ) of the neural retina, the boundary of the inner nuclear layer (INL) and the outer nuclear layer (ONL), and the retinal pigment epithelium (RPE) in the transverse section of the eye at st.35 (Fig. 3P, Q). Similar analysis with *slc7a5.L* probe was performed, and expression pattern of *slc7a5.L* was identical to that of *slc7a5.S* at stages between 10.5 and 35 (data not shown).

3.2. Inhibition of slc7a5 disrupted early neural development and interfered with eye development

To elucidate the function of slc7a5 in *Xenopus* early development, we performed loss-of-function experiments using a morpholino antisense oligonucleotide (MO). The purchased slc7a5 MO was completely complementary to *slc7a5.S* mRNA, and had three mismatches to *slc7a5.L* mRNA (Fig. 4A). Two GFP fusion constructs, *slc7a5.S-GFP* and *slc7a5.L-GFP*, were prepared to check the ability of slc7a5 MO to inhibit translation (Fig. 4B–J). While GFP fluorescence was detected in control MO injection (Fig. 4C, F, I), the fluorescence from both *slc7a5.S-GFP* and *slc7a5.L-GFP* was disappeared by slc7a5 MO (Fig. 4G, J). Thus, slc7a5 MO bound to not only *slc7a5.S* but also *slc7a5.L* mRNA to inhibit translation.

Four-cell stage embryos were unilaterally injected with 20 ng of slc7a5 MO into the dorsoanimal region. Slight left-right asymmetry of the neural fold was seen in slc7a5 MO-injected embryos at st.15 (Fig. 5A, B). Neural tube closure was completed in control MO-injected embryos at st.20 (Fig. 5C) while the neural fold in the injected side was separated from the midline in slc7a5 MO-injected embryos (88%,

Table 3
Effect of slc7a5 depletion on early neural development. Chi-square test was performed between two kinds of injected samples, control MO (20 ng) and slc7a5 MO (20 ng) or slc7a5 MO (20 ng) and slc7a5 MO (20 ng) + *slc7a5.S* (2 ng) + *slc7a5.L* (2 ng), and found to be significant, $p < 0.01$.

sox2 (st.15)

Injected sample	Normal	Reduced	Total embryos
Control MO 20 ng	110 (100%)	0 (0%)	110
slc7a5 MO 20 ng	21 (21%)	81 (79%)	102
slc7a5 MO 20 ng + *slc7a5.S* 2 ng + *slc7a5.L* 2 ng	37 (51%)	35 (49%)	72

sox2 (st.20)

Injected sample	Normal	Diffusion of *sox2*-positive region	Total embryos
Control MO 20 ng	108 (100%)	0 (0%)	108
slc7a5 MO 20 ng	4 (3%)	116 (97%)	120

xk81a1 (st.15)

Injected sample	Normal	Apparent expansion of *xk81a1*-negative region	Total embryos
Control MO 20 ng	88 (100%)	0 (0%)	88
slc7a5 MO 20 ng	18 (17%)	87 (83%)	105
slc7a5 MO 20 ng + *slc7a5.S* 2 ng + *slc7a5.L* 2 ng	36 (51%)	34 (49%)	70

xk81a1 (st.20)

Injected sample	Normal	Expansion of *xk81a1*-negative region	Total embryos
Control MO 20 ng	90 (100%)	0 (0%)	90
slc7a5 MO 20 ng	8 (7%)	112 (93%)	120

tubb2b (st.15)

Injected sample	Normal	Disappeared	Total embryos
Control MO 20 ng	93 (96%)	4 (4%)	97
slc7a5 MO 20 ng	9 (9%)	90 (91%)	99
slc7a5 MO 20 ng + *slc7a5.S* 2 ng + *slc7a5.L* 2 ng	41 (46%)	48 (54%)	89

tubb2b (st.20)

Injected sample	Normal	Disappeared	Total embryos
Control MO 20 ng	110 (99%)	1 (1%)	111
slc7a5 MO 20 ng	10 (10%)	92 (90%)	102

n = 104; Fig. 5D and Table 1). Moreover, slc7a5 depletion led to the eye defect. The mild phenotype (72%, n = 121; Fig. 5J, K and Table 1) had a smaller eye compared with that in the control side and the distinct retinal pigment was not observed in the severe phenotype (13%, n = 121; Fig. 5O, P and Table 1) at st.35. In the transverse section, the eye structures were disorganized in the slc7a5 MO-injected side to different degrees (Fig. 5L–N and Q–S). The frequency of these eye defects were significantly reduced by co-injection with rescue constructs of *slc7a5.S* and *slc7a5.L* mRNA with slc7a5-MO (mild phenotype 48%, severe phenotype 3%, n = 118; Fig. 5T–X and Table 1).

Taken together, it is suggested that slc7a5 contributes early neural and eye development in *Xenopus*.

3.3. slc7a5 inhibition disrupted normal retinal morphogenesis

To investigate eye defect caused from slc7a5 depletion in detail, expression of *pax6*, a marker for the developing retina, and *nrl* (also known as *L-maf*), a marker for the lens, were investigated at st.35. Inhibition of slc7a5 led to reduction of *pax6* and *nrl* expression (90%, n = 93 for *pax6*; 86%, n = 88 for *nrl*; Fig. 6 and Table 2). Thus, slc7a5 is likely to play a critical role in eye development.

3.4. slc7a5 depletion disrupted neural- and non-neural patterning and primary neurogenesis

Whole-mount *in situ* hybridization was performed with gene markers to examine neural development from the mid neurula (st.15) to the late neurula (st.20) in slc7a5-inhibited embryos (Fig. 7). Two markers, *sox2* (a pan neural marker) and *xk81a1* (an epidermal keratin marker), were used. Expression of *sox2* was decreased in the slc7a5 MO-injected side at st.15 (79%, n = 102; Fig. 7C and Table 3). Thereafter, the neural fold did not fuse at the midline in slc7a5-depleted embryos (97%, n = 120; Fig. 7D and Table 3). Because the *xk81a1*-negative region was expanded at st.15 (83%, n = 105; Fig. 7H and Table 3), increase in the number of epidermal cells cannot explain the decrease in neural cells. Unlike control MO-injected embryos or the uninjected side, the slc7a5 MO-injected side was not covered by epidermal cells at st.20 (93%, n = 120; Fig. 7I and Table 3). These results imply that neural tube does

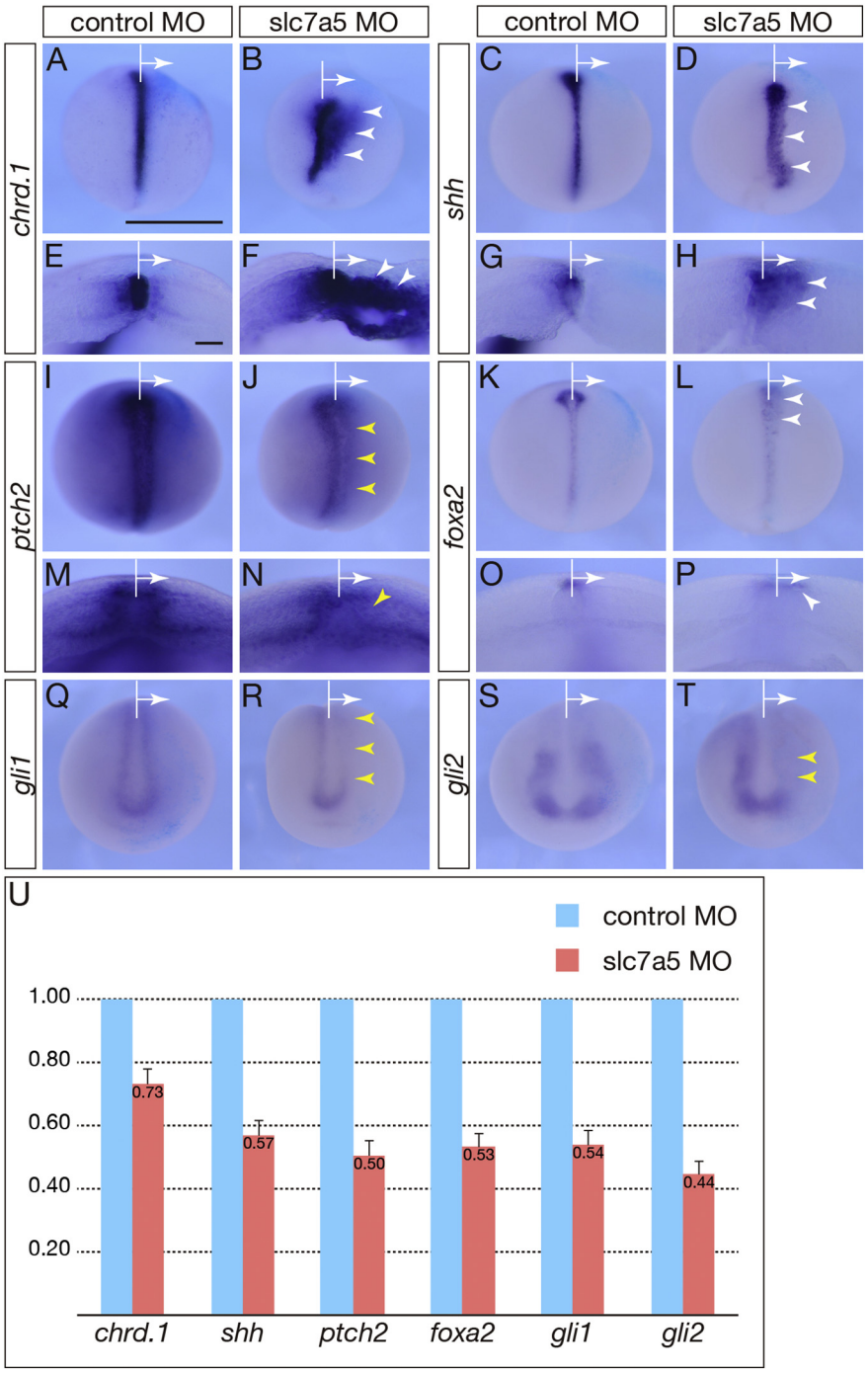

Fig. 8. Inhibition of slc7a5 disturbed notochord formation and diminished target genes in sonic hedgehog signaling.
Notochordal markers and downstream molecules in sonic hedgehog signaling were analyzed in slc7a5-depleted embryos at st.15. Arrow indicates the injected side. (A, B, E, F) *chrd.1* expression. (A, B) Dorsal view. (E, F) Transverse section. (A) Control MO-injected embryo. (B) slc7a5 MO-injected embryo. Expression of *chrd.1* was not extended enough along the anteroposterior axis and diffused laterally in slc7a5 MO-injected side (white arrowheads). (E) Transverse section of control MO-injected embryo. (F) Transverse section of slc7a5 MO-injected embryo. Expression of *chrd.1* diffused laterally (white arrowheads). (C, D, G, H) *shh* expression. (C, D) Dorsal view. (G, H) Transverse section. (C) Control MO-injected embryo. (D) slc7a5 MO-injected embryo. Faint expression of *shh* was observed similar to *chrd.1* expression (white arrowheads). (G) Transverse section of control MO-injected embryo. (H) Transverse section of slc7a5 MO-injected embryo. Expression of *shh* diffused laterally similar to *chrd.1* expression (white arrowheads). (I, J, M, N) *ptch2* expression. (I, J) Dorsal view. (M, N) Transverse section. (I) Control MO-injected embryo. (J) slc7a5 MO-injected embryo. *ptch2* was vanished in the injected side (yellow arrowheads). (M) Transverse section of control MO-injected embryo. (N) Transverse section of slc7a5 MO-injected embryo. Expression of *ptch2* was diminished in the injected side (yellow arrowhead). (K, L, O, P) *foxa2* (*HNF-3β*) expression. (K, L) Dorsal view. (O, P) Transverse section. (K) Control MO-injected embryo. (L) slc7a5 MO-injected embryo. Expression of *foxa2* was weakened in the injected side (white arrowheads). (O) Transverse section of control MO-injected embryo. (P) Transverse section of slc7a5 MO-injected embryo. Expression of *foxa2* was diffused in the injected side (white arrowhead). (Q, R) *gli1* expression. Anterior view. slc7a5 depletion impaired *gli1* expression (yellow arrowheads). (S, T) *gli2* expression. Anterior view. Expression of *gli2* was abolished in the slc7a5 MO-injected side similar to that of *gli1* (yellow arrowheads). *β-Galactosidase* RNA (1 ng) was used as a tracer. (U) RT-qPCR was performed with slc7a5-depleted embryos. Expression level of these genes was down-regulated especially in shh signaling family genes. Scale bars: 1 mm in A–D, I–L, Q–T; 0.1 mm in E–H, M–P. (For interpretation of the references to color in this figure legend, the reader is referred to the web version of this article.)

not close properly in slc7a5-depleted embryos.

To investigate whether primary neurons were established, *tubb2b* (a primary neuron marker, also known as *N-tubulin*) expression was examined. Motoneurons and interneurons were lost when slc7a5 was inhibited (91% at st.15, n = 99; 90% at st.20, n = 102; Fig. 7M, N and Table 3). These effects were reversed by coinjection with *slc7a5.S* and *slc7a5.L* rescue constructs mRNA (49%, n = 72 for *sox2*; 49%, n = 70 for *xk81a1*; 54%, n = 89 for *tubb2b*; Fig. 7E, J, O and Table 3).

Taken together, it is suggested that slc7a5 contributes to neural- and non-neural patterning and primary neuron formation in *Xenopus* development.

3.5. slc7a5 was essential for shh/gli signaling to induce proper notochordal and neural development

It has been shown that the notochord plays a key role in inducing neural tissues in animal cap assays in *Xenopus* (reviewed in Sasai and De Robertis, 1997; Kintner, 1992) and that notochordal grafts ectopically induce motoneurons (Yamada et al., 1991; Yamada et al., 1993). Given strong expression of *slc7a5* in the notochord (Fig. 3), we hypothesized that the reduction of slc7a5 protein in the notochord might compromise notochord function. Therefore, we examined notochord function mainly focused on shh pathway because it plays a central role for this induction (Patten and Placzek, 2002) (Fig. 8).

Both notochordal markers, *chrd.1* and *shh*, were detected in slc7a5 MO-injected embryos. However, the area of *chrd.1* expression spread

Table 4
Effect of slc7a5 depletion on notochord development and shh/gli signaling at st.15. Chi-square test was performed between two kinds of injected samples, control MO (20 ng) and slc7a5 MO (20 ng), and found to be significant, $p < 0.01$.

chrd.1			
Injected sample	Normal	Shortened	Total embryos
Control MO 20 ng	97 (100%)	0 (0%)	97
slc7a5 MO 20 ng	8 (6%)	116 (94%)	124

shh			
Injected sample	Normal	Shortened	Total embryos
Control MO 20 ng	79 (100%)	0 (0%)	79
slc7a5 MO 20 ng	15 (20%)	60 (80%)	75

ptch2			
Injected sample	Normal	Reduced	Total embryos
Control MO 20 ng	70 (99%)	1 (1%)	71
slc7a5 MO 20 ng	9 (13%)	60 (87%)	69

foxa2			
Injected sample	Normal	Diffused	Total embryos
Control MO 20 ng	69 (100%)	0 (0%)	69
slc7a5 MO 20 ng	12 (16%)	63 (84%)	75

gli1			
Injected sample	Normal	Reduced	Total embryos
Control MO 20 ng	71 (95%)	4 (5%)	75
slc7a5 MO 20 ng	12 (13%)	78 (87%)	90

gli2			
Injected sample	Normal	Reduced	Total embryos
Control MO 20 ng	70 (95%)	4 (5%)	74
slc7a5 MO 20 ng	10 (12%)	75 (88%)	85

laterally and shortened anteroposteriorly in slc7a5 MO-injected side (94%, n = 124; Fig. 8B, F and Table 4). Similarly, the area of *shh* expression spread laterally and shortened anteroposteriorly (80%, n = 75; Fig. 8D, H and Table 4). These results indicate that the notochord did not extend enough along anteroposterior axis in slc7a5-depleted embryos. Next, expression of *ptch2* and *foxa2*, both of which mark the notoplate (presumptive floor plate) adjacent to the notochordal tissue, was analyzed. Expression of *ptch2*, one of receptors of hedgehog, was diminished in the slc7a5 MO-injected side (87%, n = 69; Fig. 8J, N and Table 4). The area of *foxa2* (also known as *HNF-3β*) expression, a shh downstream transcription factor, was diffused (84%, n = 75; Fig. 8L, P and Table 4). Expression of *gli1* and *gli2*, target genes in shh signaling, was decreased in slc7a5-MO injected side (*gli1* reduction in 87%, n = 90; *gli2* reduction in 88%, n = 85; Fig. 7R, T and Table 4). Expression of these 6 genes, especially genes involved in shh/gli signaling, was reduced by RT-qPCR (Fig. 8U). Taken together, slc7a5 is essential for proper notochord development and shh signaling pathway.

3.6. Overexpression of slc7a5.S and slc7a5.L did not affect embryonic development

Despite the distinct phenotype by silencing *slc7a5*, overexpression of either *slc7a5.S* and/or *slc7a5.L* RNA did not show any gross abnormality in the embryos (data not shown).

4. Discussion

In this study, the expression profile of *Xenopus slc7a5* in early developmental stages was examined and loss-of-function analysis with slc7a5 MO was performed. Two genes, *slc7a5.S* and *slc7a5.L*, existed in *Xenopus laevis*. Maternal expression of *slc7a5.L* and zygotic expression of *slc7a5.S* and *slc7a5.L* were observed. *slc7a5.S* was detected in the notochord and eye anlagen at neurula stages and its expression was increased thereafter. Inhibition of slc7a5 disrupted early neural and non-neural patterning and eye development.

Recently, 68% of embryonic lethal phenotypes observed in 103 mouse gene knockout studies turn out to be due to placental defect (Perez-Garcia et al., 2018). Along the same line, embryonic lethality in *Slc7a5* knockout mice can also be explained by placental defect (Ohgaki et al., 2017). However, the study does not address the physiological functions of Slc7a5 in the placenta. Moreover, placental defect obscures the role of the gene in early stages of development. Because *Xenopus* embryos develop without a placenta, it was possible to investigate expression pattern and functional roles of this gene during early development. Our focus in this study was in neurula stages, where no other studies have addressed the role of SLC7A5 in humans or other model organism including *Xenopus*. This is the first study to our knowledge that demonstrates the role of amino acid transporter in the developmental process. As discussed later, it is likely that many of these defects

in slc7a5-depleted embryos are independent of amino acid transport function.

4.1. Inhibition of slc7a5 disrupted notochord function

Both allo-alleles of *slc7a5* showed similar spatial expression pattern in gastrula-neurula stages; they were localized at the notochord and eye field. The notochord is derived from the Spemann's organizer and secretes chordin and noggin to induce the neural plate tissue. It also secretes shh to establish the dorsoventral polarity in the neural tube (reviewed in Sasai and De Robertis, 1997). Inhibition of slc7a5 by injecting MO capable of binding to both allo-alleles (Fig. 4) resulted in shorter notochord anteroposteriorly and less restricted expression of *chrd.1* and *shh* laterally (Fig. 8A–H). In addition, the expression level of *chrd.1* in slc7a5 knockdown embryo was decreased by RT-qPCR (Fig. 8U). Thus the presumptive neural plate would be exposed to less chrd.1, a BMP inhibitor, due to lower production and dilution resulting in less inhibition of BMP signaling, which is critical for neural induction. It is likely that this disruption of chrd.1 production led to the decrease of *sox2* expression (Fig. 7A–D), a marker for neural induction, in slc7a5 MO-injected embryos.

At st.20, *tubb2b* expression that marks the motoneuron and interneuron was eliminated when slc7a5 was inhibited (Fig. 7M, N). These two kinds of primary neurons are established in the neural plate with dorsoventral polarity (Sasai and De Robertis, 1997). It is shown that shh from the notochord induces *gli1* and *gli2* in the neural plate in normal development (Ruiz i Altaba, 1998). *gli1* and *gli2* encode transcriptional factors and overexpression of these genes leads to ectopic formation of primary neurons (Brewster et al., 1998). Nguyen et al. have shown that downregulation of gli1 or gli2 with MO reduced *tubb2b* expression and they concluded that gli1 and gli2 are necessary for primary neurogenesis in *Xenopus* (Nguyen et al., 2005). In our experiments, expression of *shh* in the notochord was disrupted (Fig. 8D, H) and that of *gli1* and *gli2* was reduced when slc7a5 was inhibited with MO (Fig. 8R, T). Taken together with previous studies, loss of the motoneuron and interneuron formation in slc7a5 MO-injected embryos can be explained by the disruption of shh signaling pathway in the notochord. It should be noted, however, that primary sensory neuron formation was not affected in our experiments in contrast to Nguyen et al., where *gli1* or *gli2* inhibition leads to loss of all three primary neurons. We do not have reasonable explanation for this contradictory finding.

Expression of every gene in the notochord or the neural plate examined was down-regulated in slc7a5-depleted embryos (Fig. 8U). Interestingly, the degree of decrease in expression of shh pathway genes (*shh*, *ptch2*, *foxa2*, *gli1* and *gli2*) was more than that of *chrd.1*, suggesting that loss of slc7a5 affects more in shh signaling than chordin signaling. On the other hand, these notochord and neural plate genes still maintained ~half of their normal expression levels. Together with the fact that overexpression of slc7a5 did not show any gross defects, it is suggested that effect of slc7a5 on shh is likely to be modulatory rather than its critical determinant.

As shown in Fig. 2, *slc3a2* was not detected until late neurula stages. At least in mammals, binding of Slc7a5 to Slc3a2 is shown to be required for plasma membrane expression of Slc7a5 (Mastroberardino et al., 1998; Nakamura et al., 1999). Therefore, it is possible that slc7a5 in the notochord and the eye did not act as an amino acid transporter before *slc3a2* expression. Furthermore, when *Xenopus* embryos were cultured in the presence of JPH203, a competitive inhibitor of SLC7A5, these embryos did not show the phenotype seen in slc7a5 MO-injected embryos (Katada and Sakurai, unpublished observation), suggesting early developmental defects is independent of amino acid transport function of slc7a5.

4.2. slc7a5 and eye development

We found that slc7a5 depletion led to eye defects (Fig. 5). Many studies have shown that eye development starts with formation of the optic vesicle derived from the forebrain and is accomplished through lots of interaction between cells and molecules (reviewed in Chow and Lang, 2001). In this process, eye anlagen is specified by EFTFs (eye field transcriptional factors) such as *tbx2* (*ET*), *rax* (*Rx1*), *pax6*, *six3*, *lhx2*, *nr2e1* (*tailless*, *tll*), *six6* (*optx2*) (Zuber et al., 2003). These genes start to express in the anterior neural plate prior to st.15 (Bachy et al., 2001; Casarosa et al., 1997; Hirsch and Harris, 1997; Hollemann et al., 1998; Li et al., 1997; Mathers et al., 1997; Zhou et al., 2000; Zuber et al., 1999), when *slc7a5* expression in the eye field was barely detected. Therefore, it is likely that slc7a5 is not involved in the establishment of eye primordia, rather slc7a5 contributes to the eye development after neurula stages. Moreover, while *slc7a5* expression became more distinct as embryos grew up to st.20, *slc3a2* expression was not in the eye field during these stages. Both expression patterns of *slc7a5* and *slc3a2* were overlapped at st.25, suggesting that slc7a5 before st.20 did not function as an amino acid transporter and it did after st.25 on.

5. Conclusions

We found that amino acid transporter gene *slc7a5* is essential for notochord function of inducing neural development and for eye development in *Xenopus*. It is likely that disruption of notochord may not be related to amino acid transport. This study sheds a light on yet unexplored field of developmental function of “amino acid transporter gene”.

Acknowledgements

We appreciate Dr. Tsutomu Kinoshita (Rikkyo University, Tokyo) for providing plasmids and thank lab members for helpful advices and discussions.

References

Bachy, I., Vernier, P., Rétaux, S., 2001. The LIM-homeodomain gene family in the developing *Xenopus* brain: conservation and divergences with the mouse related to the evolution of the forebrain. J. Neurosci. 21, 7620–7629.
Brewster, R., Lee, J., Ruiz i Altaba, A., 1998. Gli/Zic factors pattern the neural plate by defining domains of cell differentiation. Nature 393, 579–583.
Casarosa, S., Andreazzoli, M., Simeone, A., Barsacchi, G., 1997. *Xrx1*, a novel *Xenopus* homeobox gene expressed during eye and pineal gland development. Mech. Dev. 61, 187–198.
Chow, R.L., Lang, R.A., 2001. Early eye development in vertebrates. Annu. Rev. Cell Dev. Biol. 17, 255–296.
Chrostowski, M.K., McGonnigal, B.G., Stabila, J.P., Padbury, J.F., 2009. LAT-1 expression in pre- and post-implantation embryos and placenta. Placenta 30, 270–276.
Cormerais, Y., Giuliano, S., LeFloch, R., Front, B., Durivault, J., Tambutté, E., Massard, P.A., de la Ballina, L.R., Endou, H., Wempe, M.F., Palacin, M., Parks, S.K., Pouyssegur, J., 2016. Genetic distribution of the multifunctional CD98/LAT1 complex demonstrates the key role of essential amino acid transport in the control of mTORC1 and tumor growth. Cancer Res. 76, 4481–4492.
Hirsch, N., Harris, W.A., 1997. *Xenopus* Pax-6 and retinal development. J. Neurobiol. 32, 45–61.
Hollemann, T., Bellefroid, E., Pieler, T., 1998. The *Xenopus* homologue of the *Drosophila* gene *tailless* has a function in early eye development. Development 125, 2425–2432.
Kanai, Y., Segawa, H., Ki, Miyamoto, Uchino, H., Takeda, E., Endou, H., 1998. Expression cloning and characterization of a transporter for large neutral amino acids activated by the heavy chain of 4F2 antigen (CD98). J. Biol. Chem. 273, 23629–23632.
Katada, T., Sakurai, H., 2016. Proper Notch activity is necessary for the establishment of proximal cells and differentiation of intermediate, distal, and connecting tubule in *Xenopus* pronephros development. Dev. Dyn. 245, 472–482.
Kim, C.S., Cho, S.H., Chun, H.S., Lee, S.Y., Endou, H., Kanai, Y., Kim, D.K., 2008. BCH, an inhibitor of system L amino acid transporters, induces apoptosis in cancer cells. Biol. Pharm. Bull. 31, 1096–1100.
Kimball, S.R., Jefferson, L.S., 2004. Molecular mechanisms through which amino acids mediate signaling through the mammalian target of rapamycin. Curr. Opin. Clin. Nutr. Metab. Care 7, 39–44.
Kintner, C., 1992. Molecular basis of early neural development in *Xenopus* embryos. Annu. Rev. Neurosci. 15, 251–284.
Koga, M., Kudoh, T., Hamada, Y., Watanabe, M., Kageura, H., 2007. A new triple staining method for double *in situ* hybridization in combination with cell lineage tracing in whole-mount *Xenopus* embryos. Develop. Growth Differ. 49, 635–645.
Li, H., Tierney, C., Wen, L., Wu, J.Y., Rao, Y., 1997. A single morphogenetic field gives rise to two retina primordia under the influence of the prechordal plate. Development

124, 603–615.
Mastroberardino, L., Spindler, B., Pfeiffer, R., Skelly, P.J., Loffing, J., Shoemaker, C.B., Verrey, F., 1998. Amino-acid transport by heterodimers of 4F2hc/CD98 and members of a permease family. Nature 395, 288–291.
Mathers, P.H., Grinberg, A., Mahon, K.A., Jamrich, M., 1997. The *Rx* homeobox gene is essential for vertebrate eye development. Nature 387, 603–607.
Mayor, R., Morgan, R., Sargent, M.G., 1995. Induction of the prospective neural crest of *Xenopus*. Development 121, 767–777.
Nakada, N., Mikami, T., Hana, K., Ichinoe, M., Yanagisawa, N., Yoshida, T., Endou, H., Okayasu, I., 2014. Unique and selective expression of L-amino acid transporter 1 in human tissue as well as being an aspect of oncofetal protein. Histol. Histopathol. 29, 217–227.
Nakamura, E., Sato, M., Yang, H., Miyagawa, F., Harasaki, M., Tomita, K., Matsuoka, S., Noma, A., Iwai, K., Minato, N., 1999. 4F2 (CD98) heavy chain is associated covalently with an amino acid transporter and controls intracellular trafficking and membrane topology of 4F2 heterodimer. J. Biol. Chem. 274, 3009–3016.
Nguyen, V., Chokas, A.L., Stecca, B., Ruiz i Altaba, A., 2005. Cooperative requirement of the Gli proteins in neurogenesis. Development 132, 3267–3279.
Nieuwkoop, P.D., Faber, J., 1994. Normal Table of *Xenopus laevis* (Daudin). Garland Publishing Inc., New York.
Oda, K., Hosoda, N., Endo, H., Saito, K., Tsujihara, K., Yamamura, M., Sakata, T., Anzai, N., Wempe, M.F., Kanai, Y., Endou, H., 2010. L-type amino acid transporter 1 inhibitors inhibit tumor cell growth. Cancer Sci. 101, 173–179.
Ohgaki, R., Ohmori, T., Hara, S., Nakagomi, S., Kanai-Azuma, M., Kaneda-Nakashima, K., Okuda, S., Nagamori, S., Kanai, Y., 2017. Essential roles of L-type amino acid transporter 1 in syncytiotrophoblast development by presenting fusogenic 4F2hc. Mol. Cell. Biol. 37, e00427-16.
Patten, I., Placzek, M., 2002. Opponent activities of Shh and BMP signaling during floor plate induction in vivo. Curr. Biol. 12, 47–52.
Perez-Garcia, V., Fineberg, E., Wilson, R., Murray, A., Mazzeo, C.I., Tudor, C., Sienerth, A., White, J.K., Tuck, E., Ryder, E.J., Gleeson, D., Siragher, E., Wardle-Jones, H., Staudt, N., Wali, N., Collins, J., Geyer, S., Busch-Nentwich, E.M., Galli, A., Smith, J.C., Robertson, E., Adams, D.J., Weninger, W.J., Mohun, T., Hemberger, M., 2018. Placentation defects are highly prevalent in embryonic lethal mouse mutants. Nature 555, 463–468.
Poncet, N., Mitchell, F.E., Ibrahim, A.F., McGuire, V.A., English, G., Arthur, J.S., Shi, Y.B., Taylor, P.M., 2014. The catalytic subunit of the system L1 amino acid transporter (*Slc7a5*) facilitates nutrient signalling in mouse skeletal muscle. PLoS One 9, e89547.
Prasad, P.D., Wang, H., Huang, W., Kekuda, R., Rajan, D.P., Leibach, F.H., Ganapathy, V., 1999. Human LAT1, a subunit of system L amino acid transporter: molecular cloning and transport function. Biochem. Biophys. Res. Commun. 255, 283–288.
Rosilio, C., Nebout, M., Imbert, V., Griessinger, E., Neffati, Z., Benadiba, J., Hagenbeek, T., Spits, H., Reverso, J., Ambrosetti, D., Michiels, J.F., Bailly-Maitre, B., Endou, H., Wempe, M.F., Peyron, J.F., 2015. L-type amino-acid transporter 1 (LAT1): a therapeutic target supporting growth and survival of T-cell lymphoblastic lymphoma/T-cell acute lymphoblastic leukemia. Leukemia 29, 1253–1266.
Ruiz i Altaba, A., 1998. Combinatorial *Gli* gene function in floor plate and neuronal inductions by Sonic hedgehog. Development 125, 2203–2212.
Sakata, T., Ferdous, G., Tsuruta, T., Satoh, T., Baba, S., Muto, T., Ueno, A., Kanai, Y., Endou, H., Okayasu, I., 2009. L-type amino-acid transporter 1 as a novel biomarker for high-grade malignancy in prostate cancer. Pathol. Int. 59, 7–18.
Sasai, Y., De Robertis, E.M., 1997. Ectodermal patterning in vertebrate embryos. Dev. Biol. 182, 5–20.
Shain, D.H., Zuber, M.X., 1996. Sodium dodecyl sulfate (SDS)-based whole-mount in situ hybridization of *Xenopus laevis* embryos. J. Biochem. Biophys. Methods 31, 185–188.
Sinclair, L.V., Rolf, J., Emslie, E., Shi, Y.B., Taylor, P.M., Cantrell, D.A., 2013. Control of amino-acid transport by antigen receptors coordinates the metabolic reprogramming essential for T cell differentiation. Nat. Immunol. 14, 500–508.
Ueno, S., Kimura, T., Yamaga, T., Kawada, A., Ochiai, T., Endou, H., Sakurai, H., 2016. Metformin enhances anti-tumor effect of L-type amino acid transporter 1 (LAT1) inhibitor. J. Pharmacol. Sci. 131, 110–117.
Wagner, C.A., Lang, F., Bröer, S., 2001. Function and structure of heterodimeric amino acid transporters. Am. J. Phys. Cell Physiol. 281, 1077–1093.
Yamada, T., Placzek, M., Tanaka, H., Dodd, J., Jessell, T.M., 1991. Control of cell pattern in the developing nervous system: polarizing activity of the floor plate and notochord. Cell 64, 635–647.
Yamada, T., Pfaff, S.L., Edlund, T., Jessell, T.M., 1993. Control of cell pattern in the neural tube: motor neuron induction by diffusible factors from notochord and floor plate. Cell 73, 673–686.
Yanagisawa, N., Ichinoe, M., Mikami, T., Nakada, N., Hana, K., Koizumi, W., Endou, H., Okayasu, I., 2012. High expression of L-type amino acid transporter 1 (LAT1) predicts poor prognosis in pancreatic ductal adenocarcinomas. J. Clin. Pathol. 65, 1019–1023.
Yun, D.W., Lee, S.A., Park, M.G., Kim, J.S., Yu, S.K., Park, M.R., Kim, S.G., Oh, J.S., Kim, C.S., Kim, H.J., Kim, J.S., Chun, H.S., Kanai, Y., Endou, H., Wempe, M.F., Kim, D.K., 2014. JPH203, an L-type amino acid transporter 1-selective compound, induces apoptosis of YD-38 human oral cancer cells. J. Pharmacol. Sci. 124, 208–217.
Zhou, X., Hollemann, T., Pieler, T., Gruss, P., 2000. Cloning and expression of *xSix3*, the *Xenopus* homologue of murine *Six3*. Mech. Dev. 91, 327–330.
Zuber, M.E., Perron, M., Philpott, A., Bang, A., Harris, W.A., 1999. Giant eyes in *Xenopus laevis* by overexpression of *XOptx2*. Cell 98, 341–352.
Zuber, M.E., Gestri, G., Viczian, A.S., Barsacchi, G., Harris, W.A., 2003. Specification of the vertebrate eye by a network of eye field transcription factors. Development 130, 5155–5167.